



**HAL**  
open science

## Spatial patterns and trends of extreme rainfall over the southern coastal belt of West Africa

Marc Kpanou, Patrick Laux, Télésphore Brou, Expédit Vissin, Pierre Camberlin, Pascal Roucou

► **To cite this version:**

Marc Kpanou, Patrick Laux, Télésphore Brou, Expédit Vissin, Pierre Camberlin, et al.. Spatial patterns and trends of extreme rainfall over the southern coastal belt of West Africa. *Theoretical and Applied Climatology*, 2021, 143, pp.473-487. 10.1007/s00704-020-03441-8 . hal-04648360

**HAL Id: hal-04648360**


**<https://cnrs.hal.science/hal-04648360v1>**

Submitted on 15 Jul 2024

**HAL** is a multi-disciplinary open access archive for the deposit and dissemination of scientific research documents, whether they are published or not. The documents may come from teaching and research institutions in France or abroad, or from public or private research centers.

L'archive ouverte pluridisciplinaire **HAL**, est destinée au dépôt et à la diffusion de documents scientifiques de niveau recherche, publiés ou non, émanant des établissements d'enseignement et de recherche français ou étrangers, des laboratoires publics ou privés.

# Spatial patterns and trends of extreme rainfall over the southern coastal belt of West Africa

Marc Kpanou<sup>1,2</sup>  · Patrick Laux<sup>4</sup> · Téléphore Brou<sup>3</sup> · Expédit Vissin<sup>2</sup> · Pierre Camberlin<sup>1</sup> · Pascal Roucou<sup>1</sup>

Received: 22 November 2018 / Accepted: 15 October 2020

## Abstract

The southern coastal belt of West Africa (SCWA) with its high population density and many major cities, combined to the low elevation and poor urban planning, is very vulnerable to floods resulting from extreme rainfall events. The aim of this paper is to analyze the characteristics of extreme rainfall in the SCWA during the 1981–2015 period, in terms of frequency, intensity, seasonality, and trends. Therefore, daily rainfall of 31 stations located in the southern part of Côte d'Ivoire, Ghana, Togo, and Benin and rainfall estimation products combining in situ observations and satellites rainfall estimation data have been used. For each station and pixel, the local 95th percentile (P95) computed on all rain days of at least 1 mm was used to define extreme rainfall events. Rainfall on the coastal belt is heavier than further inland, with P95 values reaching 82 and 52 mm/day for coastal and continental stations, respectively. Extreme rainfall along the coast occurs predominantly between May and July. Interannual variations of different indicators of extreme rainfall show a broad agreement between rain gauge data and rainfall estimates from CHIRPS (Climate Hazards Group InfraRed Precipitation with Station) data. In the southern part of Côte d'Ivoire and Togo/Benin, increase of number of extreme rainfall event (NP95) and stability number of days with rainfall less than P95 (NL95) are recorded, which induces an increase of total rainfall. But, in the southern part of Ghana, there is a stable total rainfall due to an increase in NP95 compensated by a decrease in NL95.

**Keywords** Extreme rainfall · Trend · West Africa · Coastal belt

## 1 Introduction

Extreme rainfall events in the southern coastal part of West Africa (SCWA) constitute a major hazard. The low elevation combined to poor urban planning and high population densities participate to flood damages. As much as 30.1% of the total population of the coastal states of Côte d'Ivoire, Ghana, Togo, and Benin is concentrated in a 40-km-wide corridor

bordering the Atlantic Ocean (GPW data, CIESIN 2015). All the major cities in the region are recurrently hit by flooding. The flood that hit Accra in June 2015 affected around 53,000 people in the city and caused an estimated US\$100 million in damages (Erman et al. 2018). During the night of June 30 to July 1, 2014, between 5 am and 6 am, 85 mm of rain was recorded at the Abidjan station. On June 2, 3, 4, and 5, 2015, 210 mm and 257 mm of rain were recorded

---

✉ Marc Kpanou  
mackpanou@yahoo.fr

Patrick Laux  
patrick.laux@kit.edu

Téléphore Brou  
telesphore.brou@univ-reunion.fr

Expédit Vissin  
exlaure@gmail.com

Pierre Camberlin  
pierre.camberlin@u-bourgogne.fr

Pascal Roucou  
pascal.roucou@u-bourgogne.fr

- <sup>1</sup> Centre de Recherche de Climatologie, Biogéosciences, Université Bourgogne Franche – Comté, 6 Bd Gabriel, 21000 Dijon, France
- <sup>2</sup> Laboratoire Pierre PAGNEY: Climat, Eau, Ecosystèmes et Développement, Université d'Abomey-Calavi, 01 BP 526 Cotonou, Bénin
- <sup>3</sup> Département de Géographie / UMR 228 Espace-Dev, Université de La Réunion, Saint-Denis, France
- <sup>4</sup> Institute of Meteorology and Climate Research, Karlsruhe Institute of Technology, Karlsruhe, Germany

respectively at the Cotonou and Abidjan stations. And on June 10, 2016, 184 mm of rain was recorded at the Accra station. These few examples suggest that extreme precipitation on the coast facing the Gulf of Guinea is very frequent at the peak of the main rains in June. In the rural zone, flooding caused by extreme rainfall disrupts agricultural activities and is liable to the destruction of crops. Combined with the risk related to sea-level rise, a future increase in extreme rainfall events would have serious implications in coastal West Africa. According to the Fifth IPCC report, extreme precipitation and drought episodes will very likely become more extreme and more frequent, which could have harmful effects on natural and human systems (IPCC 2013).

Hence, a better understanding of extreme rainfall space-time variability and trend in the SCWA is an important challenge. Observed trends of extreme rainfall tend to vary seasonally and regionally (Groisman et al. 2005). While at global scale many regions have shown an increase in extreme precipitation over the last half century, parts of central Africa showed a decrease (Aguilar et al. 2009). Furthermore, initial studies on southern and western Africa found no consistent spatial patterns of trends in heavy precipitation events (New et al. 2006).

In West Africa, Chaney et al. (2014), analyzing rainfall trends between 1979 and 2004, mostly found increases in total rainfall recorded on days with heavy rains, but significant only in part of the Sahel as a result of recovery from droughts of the 1970s and 1980s. Using an integrated regional approach, Panthou et al. (2014) indicated that the Sahelian rainfall regime is characterized by a lasting deficit of the numbers of rainy days, while at the same time, the extreme rainfall has increased from 1970 to 2010. Comparable results were obtained by Mouhamed et al. (2013). Sanogo et al. (2015) pointed out an increase in both the frequency and intensity of extreme rainfall (exceeding the 95% percentile) in the Sahel in the 1980–2010 period, but over the Guinea Coast, only the intensity of extreme rainfall showed a significant increase. Barry et al. (2018) analyzed West Africa climate extremes over the same period. They noticed a significant increase of the frequency and intensity of extreme rainfall at regional scale, but in the Guinean region, changes are non-homogenous. While variations in the frequency and intensity of extreme rainfall in the Sahel or over West Africa as a whole have been documented, only few studies have analyzed extreme precipitation along the southern coastal part of West Africa. Some studies have considered rainfall trends in Côte d'Ivoire (Goula et al. 2012; Soro et al. 2016; Ta et al. 2016), in Ghana (Neumann et al. 2007; Manzanas et al. 2014), or Benin (Yabi and Afouda 2012; Panthou et al. 2014; Ague and Afouda 2015), but not specifically in their coastal part. Goula et al. (2012), Ague and Afouda (2015), and Soro et al. (2016) fitted different extreme value distributions such as GEV, Gumbel, Lognormal,

Pearson type III, and Log-Pearson type III to rainfall extremes and modelled annual maximum daily rainfall by a PARETO distribution. Goula et al. (2012) found in the 1942–2002 period a small number of stations (29% of total station of Côte d'Ivoire) recording a significative decrease in the number of days receiving more than 50 mm. Manzanas et al. (2014) found in the 1986–2010 period an increase (but not statistically significant) of extreme rainfall events in southern of Ghana.

The detection of extreme rainfall trends depends on the availability of rainfall data at adequate spatial and temporal scales. In West Africa, conventional rain gauges have been the main source of rainfall data (Panthou et al. 2014). However, getting a consistent rainfall record from weather observing stations unevenly distributed is a main challenge in developing countries such as Benin, Togo, Ghana, and Côte d'Ivoire. Moreover, documenting the space-time patterns of rainfall variability, particularly its extremes, over a region with strong spatial gradients such as the SCWA, may require the use of gridded, high-resolution datasets (Chaney et al. 2014).

Satellite rainfall estimates (SRE) may provide information with high spatiotemporal resolution over widespread regions where conventional rainfall data are scarce or absent (Su et al. 2008; Li et al. 2010). In the recent years, many intercomparison studies of SRE products have been carried out, especially over Africa.

Toté et al. (2015) compared three gridded satellite rainfall products to independent gauge data in Mozambique during the 2001–2012 period. Their study indicates that during the cyclone season, Climate Hazard Group InfraRed Precipitation with Stations (CHIRPS) shows the best results. Seven operational high-resolution satellite-based rainfall products have been compared to independent gauge data in Burkina Faso over the 2001–2014 period (Dembélé and Zwart 2016). They conclude that Precipitation Estimation from Remotely Sensed Information using Artificial Neural Networks (PERSIANN) and CHIRPS are adequate for flood monitoring. Trejo et al. (2016) made comparison between CHIRPS and gauge data in Venezuela for the 1981–2007 period in considering different rainfall categories, seasonality, and spatial context. The results show that CHIRPS achieved better performances during the rainy season (April–September). Also, the product shows best overall performance over flat and open regions, where precipitation is influenced by the Intertropical Convergence Zone activity and local convective systems. Bayissa et al. (2017) evaluated five satellite rainfall products in comparison with ground observation data in the Upper Blue Nile Basin in Ethiopia for the 1998–2015 period. It appears that CHIRPS rainfall shows good accordance with gauge data. However, only a small number of SRE intercomparison studies considered statistics of extreme rainfall (e.g. Herold et al. (2017) for tropical land areas; Katsanos et al. (2016) and Zittis et al. (2017) for Cyprus; Bai et al. (2018) for China).

In this paper, we assess the accuracy of three RSE products to detect extreme rainfall by comparing them with gauge rainfall over the years 1981–2001. We then analyze the space-time patterns of extreme rainfall variability along the southern coastal belt of West Africa, and finally examine the trend in the frequency and intensity of extreme rainfall using both rain gauge and selected SRE in the 1981–2015 period.

We hypothesize that the SCWA singularizes from the rest of Guinean West Africa in terms of extreme rainfall hazards. The following questions will therefore be considered: (i) How much do the frequency and seasonality of extreme rainfall events in the coastal region demarcate from those of inland regions? (ii) What is the contribution of the extreme events to seasonal and annual precipitation amounts in the SCWA? (iii) Are there any significant trends in the occurrence of extreme events and their contribution to annual rainfall along the coast since the 1980s, and how do they compare to the trends found in the rest of West Africa?

To answer these questions, the paper is organized as follows: Section 2 presents the data used in the study; the methods and indices calculation are described in “Section 3”; “Section 4” presents the results; finally, the discussion and conclusion are presented in “Section 5”.

## 2 Data

Two kinds of daily rainfall data have been used: rain gauge observations and gridded estimations from satellite remote sensing.

Concerning rain gauge observations, daily rainfall has been collected for 38 stations located in the meridional part of Côte d’Ivoire, Ghana, Togo, and Benin (Fig. 1 and Table 1). This includes both coastal stations and inland stations up to a distance of about 200 km from the coast (i.e. reaching about 7° N for Côte d’Ivoire and 8° N for Benin).

The reason of this choice is that while the focus is on the coast belt (where there is a high concentration of people, and where we hypothesize a higher intensity of rainfall), it is desirable to show how much this coastal belt differentiates from inland areas in terms of frequency of extreme rainfall events, interannual variability, and trends. The region retained is characterized by a Guinean rainfall regime (two rainy seasons, see below), while the region beyond these latitudes (7 to 8° N) experiences Sudanian and Sahelian rainfall regimes characterized by only one rainy season.

The observed daily rainfall data from 1981 to 2015 for these 38 stations were obtained from the Société d’Exploitation et de Développement Aéroportuaire, Aéronautique et Météorologie (Côte d’Ivoire), Ghana Meteorological Agency, Direction Générale de la Météorologie Nationale (Togo), and the Agence Nationale de la Météorologie (METEO-Bénin). They were combined with additional data from GHCN (Global

Historical Climate Network, Menne et al. (2012)). Records dating back to 1951 or 1961 are available for several stations, but we focus in the recent period 1981–2015 because it was shown to display a consistent trend over parts of West Africa in previous studies (Manzanas et al. 2014; Barry et al. 2018) and because SRE also enable to document this period.

A pre-processing has been done to set apart years and stations which contained too much missing data to infer interannual statistics on extreme rainfall. An upper threshold was fixed at 36 missing days per year (10% of the yearly data). If 1 year recorded 36 days (or more) of missing data, this year was disqualified and all the data for this year were set to missing. The number of non-missing years for each station is then assessed. Thirty-one stations which got less than 20% of missing years are finally retained for the comparison study with the satellite rainfall estimations.

A brief description of the two gridded satellite rainfall estimations (SRE) that are compared to gauge data in this study is given below: (1) the Climate Hazards Group InfraRed Precipitation with Stations (CHIRPS) dataset; (2) the Precipitation Estimation from Remotely Sensed Information using Artificial Neural Networks for Climate Data Record (PERSIANN-CDR) dataset.

CHIRPS is produced by the Climate Hazards Group under the umbrella of USGS and of Earth Resources Observation and Science (EROS) centre. The CHIRPS processing and validation includes four steps (Funk et al. 2015): (1) create a historical precipitation climatology (CHPclim) from station normals and satellite means (observation satellites and Tropical Rainfall Measuring Mission (TRMM)); (2) create a daily anomaly precipitation estimates from cold cloud duration as a fraction of long-term mean cold cloud duration (Precipitation%); (3) multiply Precipitation% by CHPclim to obtain CHIRP; (4) blend in gauge observations (GHCN (Global Historical Climatology Network), GSOD (Global Surface Summary of the Day), and GTS (Global Telecommunication System)) with CHIRP to make CHIRPS. CHIRPS is gridded at  $0.05^\circ \times 0.05^\circ$  (about 6 km of resolution). The data start from 1981 and are updated until now. For this study, daily rainfall data are extracted in the 1981–2015 period.

PERSIANN-CDR is developed by the Center for Hydrometeorology and Remote Sensing (CHRS) at the University of California, Irvine (UCI) (Novella and Thiaw 2010). The PERSIANN algorithm uses an artificial neural network model to estimate precipitation using infrared satellite data (Zambrano-Bigiarini et al. 2017). The PERSIANN-CDR was developed by applying the PERSIANN algorithm to Gridded Satellite Infrared Data (GridSat-B1) and then bias-correcting estimations using  $2.5^\circ$  monthly Global Precipitation Climatology Project (GPCP v2.2) precipitation data (Ashouri et al. 2015). PERSIANN-CDR provides near-global ( $60^\circ$  S– $60^\circ$  N) daily precipitation data at  $0.25^\circ$  spatial resolution since 1983.

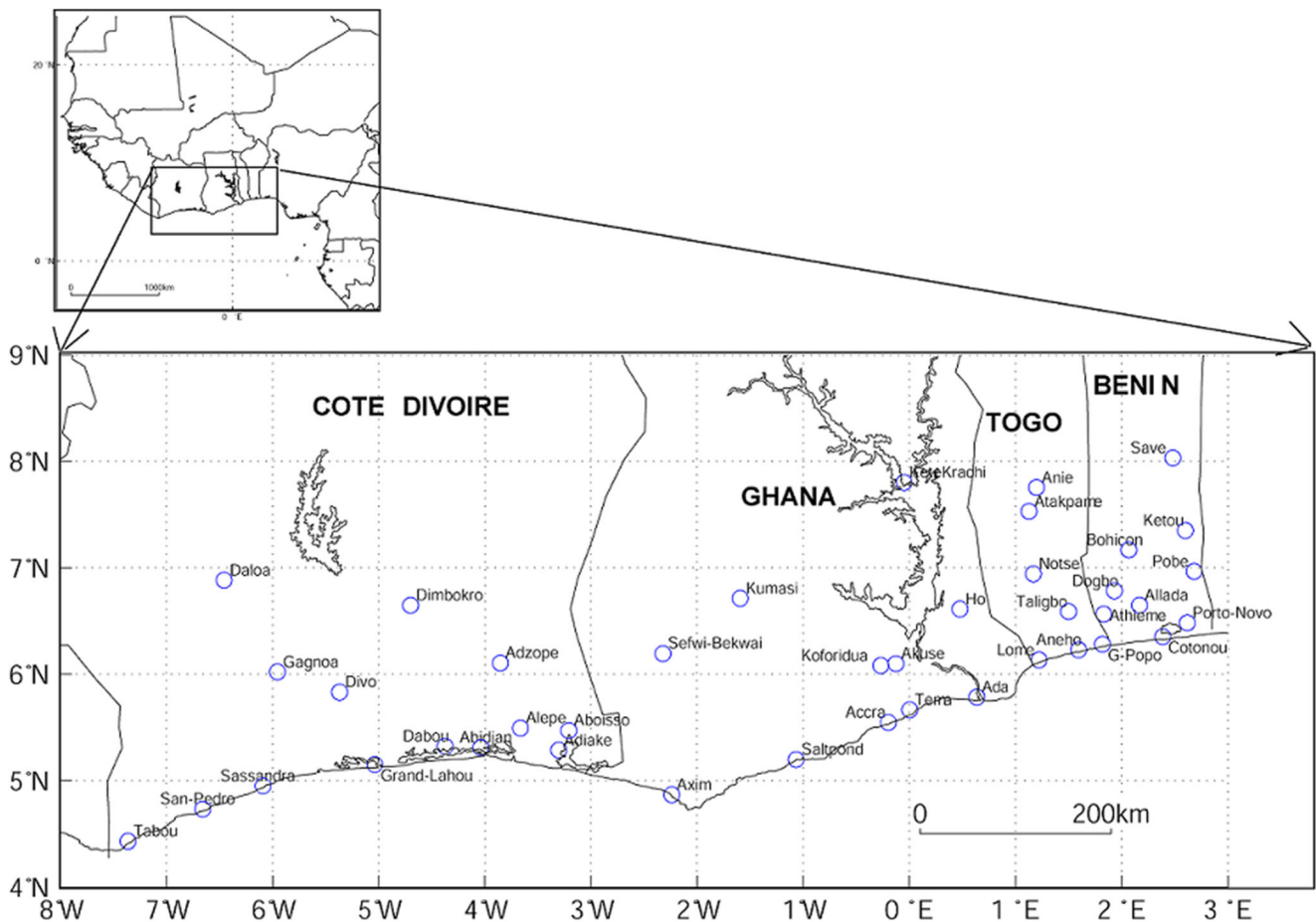


Fig. 1 The location of the study area. Circles denote the location of the weather stations used

### 3 Methodology

#### 3.1 Definition of extreme rainfall statistics

An extreme rainfall day could be defined in function of a fixed threshold (in millimetres) or based on the distribution of daily data at each station. The first method is not adapted to this work, first because it cannot take into account the rainfall variability between the different areas and second because a single threshold cannot be used for observations and SRE since we expect possible systematic biases in the satellite estimations. Here, following the recommendations of the Expert Team on Climate Change Detection and Indices (ETCCDI) (Zhang et al. 2011) we defined an extreme rainy event as a day where rainfall recorded is higher than or equal to the local 95th percentile (P95) of all rainy day. A rainy day is considered a day which recorded a rainfall of at least 1 mm (WMO 2009).

P95 values have been computed for each rainfall station and each pixel from the selected SRE, based on all available data at daily scale. From this, four other parameters have been derived:

- NP95: The number of days with rainfall greater than or equal to P95;

- PP95: The percentage rainfall amount on extreme rainfall days (rainfall  $\geq$  P95) compared to the total annual rainfall;
- NL95: The number of days with rainfall less than P95 (NL95);
- PL95: The percentage of total rainfall on days receiving less than P95 (rainfall  $<$  P95) compared to the total annual rainfall.

A validation of the SRE data will be carried out by comparing the P95 values in the SRE and at the stations. As there are many missing data during 2001–2015 for several stations, long-term rainfall trends will be analyzed based on the selected SRE data, which cover the 35-year period 1981–2015. Prior to that, a second validation of the selected SRE will be assessed by comparing the interannual variations of total rainfall, NP95, and PP95 in SRE with observed data over a shorter common period (1981–2000). The comparison is based on the spatial patterns and time series obtained from principal component analyses of annual values of these indicators, for rain gauge stations and selected SRE grid points corresponding to each station. Only the stations having less than 20% missing years are retained at this stage (Table 1).

**Table 1** Geographical of location, available period, missing data for each station. Asterisks indicate coastline stations. Stations selected for the rainfall trends study are written in italics

Countries	Stations	Latitude	Longitude	Percent missing days for 1981–2015 period	Percent missing days for 1981–2001 period
Côte d'Ivoire	<i>Abidjan*</i>	5.3133	−4.0372	11.4	9.5
Côte d'Ivoire	<i>Aboisso*</i>	5.4747	−3.2097	45.7	9.5
Côte d'Ivoire	<i>Adiaké*</i>	5.2858	−3.3042	28.6	4.8
Côte d'Ivoire	<i>Adzopé</i>	6.1069	−3.8600	45.7	9.5
Côte d'Ivoire	<i>Alépé</i>	5.4967	−3.6631	51.4	19.0
Côte d'Ivoire	<i>Dabou*</i>	5.3256	−4.3719	-	28.6
Côte d'Ivoire	<i>Daloa</i>	6.8828	−6.4536	-	19.0
Côte d'Ivoire	<i>Dimbokro</i>	6.6503	−4.6997	25.7	4.8
Côte d'Ivoire	<i>Divo</i>	5.8331	−5.3675	-	4.8
Côte d'Ivoire	<i>Gagnoa</i>	6.0186	−5.9514	25.7	4.8
Côte d'Ivoire	<i>Grand-Lahou*</i>	5.1353	−5.0350	-	19.0
Côte d'Ivoire	<i>San-Pedro*</i>	4.7333	−66.583	60	66.7
Côte d'Ivoire	<i>Sassandra*</i>	4.9500	−6.0917	22.9	4.8
Côte d'Ivoire	<i>Tabou*</i>	4.4314	−7.3606	22.9	4.8
Ghana	<i>Accra*</i>	5.5497	−0.2006	–	0.0
Ghana	<i>Ada*</i>	5.7836	0.6331	–	0.0
Ghana	<i>Akuse</i>	6.0992	−0.1275	–	0.0
Ghana	<i>Axim*</i>	4.8664	−2.2408	–	0.0
Ghana	<i>Ho</i>	6.6108	0.4781	–	9.5
Ghana	<i>Kete-Krachi</i>	7.8017	−0.0514	–	9.5
Ghana	<i>Koforidua</i>	6.0789	−0.2714	–	0.0
Ghana	<i>Kumasi</i>	6.7133	−1.5917	–	0.0
Ghana	<i>Saltpond*</i>	5.2000	−1.0667	–	0.0
Ghana	<i>Sefwi-Bekwai</i>	6.1947	−2.3228	–	0.0
Ghana	<i>Tema*</i>	6.5872	−0.0003	–	0.0
Togo	<i>Aného*</i>	6.2294	1.5961	46.8	14.3
Togo	<i>Anié</i>	7.7508	1.1981	0.0	0.0
Togo	<i>Lomé*</i>	6.1322	1.2225	94.3	95.2
Togo	<i>Notse</i>	6.9461	1.1689	42.9	42.9
Togo	<i>Taligbo</i>	6.5872	1.5019	2.9	0.0
Benin	<i>Ketou</i>	7.3500	2.6000	5.7	0.0
Benin	<i>Bohicon</i>	7.1667	2.0667	0.0	0.0
Benin	<i>Pobè</i>	6.9667	2.6833	11.4	9.5
Benin	<i>Dogbo</i>	6.7500	1.7833	28.6	23.8
Benin	<i>Allada</i>	6.6500	2.1333	65.7	47.6
Benin	<i>Porto-Novo*</i>	6.4833	2.6167	5.7	0.0
Benin	<i>Cotonou*</i>	6.3500	2.3833	0.0	0.0
Benin	<i>Grand-Popo*</i>	6.2833	1.8167	17.1	4.8

In order to analyze the space-time patterns, as the datasets still contain some missing years, we used probabilistic principal component analysis (PPCA) which enables to work on incomplete time series (Tipping and Bishop 1999; Lopes et al. 2016). The PPCA is based on a latent variable model, which is established on available data only. The PPCA first reconstructs missing data, and the quality of reconstruction is tested using a

Monte Carlo approach. A set of 10% missing entries are randomly created by year-station blocks separately for NP95 and PP95. The PPCA is next used to estimate these data from the eigenvector computed on the available entries only. The skill of the reconstructions is computed as the correlation between reconstructed and observed indices related to the 95th percentile of NP95 and PP95 (Moron et al. 2016).

## 3.2 Evaluation of satellite rainfall estimations

In this work, the evaluation of the SRE has been carried out over the period 1981 to 2015 for CHIRPS and 1983 to 2015 for PERSIANN, using measured rainfall data from 31 independent weather stations. Evaluation with independent data set is essential to determine how well the SRE reproduces extreme rainfall at daily scale.

Firstly, we extracted the daily rainfall data from SRE grid points corresponding to each rain gauge. Secondly, bias and root mean square error (RMSE) were used to compare the satellite estimates of rainfall to the rain gauge data, as in Adler and Negri (1988), Toté et al. (2015), Dembélé and Zwart (2016), Trejo et al. (2016), and Bayissa et al. (2017). Bias and RMSE are respectively calculated according to the following formulas:

$$\text{BIAS} = \sum_{i=1}^n (S_i - G_i), \text{RMSE} = \sqrt{\frac{1}{n} \sum_{i=1}^n (S_i - G_i)^2}.$$

$S_i$  and  $G_i$  designate satellite rainfall estimate and gauge rainfall measurements, respectively. The bias reflects how well the mean of satellite rainfall corresponds with the mean of the observed rainfall. A bias value close to zero indicates that the cumulative SRE is closer to the cumulative observed rainfall. The RMSE is used to measure the average magnitude of the estimated errors between the satellite rainfall and the observed rainfall. A lower RMSE value means that SRE and observations are close to each other.

## 3.3 Trend analysis

Tests for detection of significant trends in climate time series can be classified as parametric and nonparametric methods. Parametric trend test require data to be independent and normally distributed, while nonparametric trend tests require only that the data to be independent (Gocic and Trajkovic 2013). Here, Mann-Kendall's statistic (Mann 1945; Kendall 1975) and Sen's slope estimator (Sen 1968) were used respectively to test the statistical significance of the trends and to estimate the magnitude of the trends in the rainfall variables. Odoulami and Akinsanola (2017) also applied the two methods on gridded datasets for West Africa.

## 4 Results

### 4.1 Comparison between satellite rainfall estimations and rain gauge data

In this study, two satellite rainfall products were investigated to identify the best product to use for spatial patterns and trends of extreme rainfall over the study area in the 1981–2015 period. Area-averaged (over 31 stations) P95 values for satellite rainfall estimations and rain gauge data over the period 1981–2015 are presented in Table 2.

**Table 2** Area-averaged values of P95 (mm/day) at the 31 stations (OBS) and the nearest grid-point of three rainfall estimation products (PERSIANN and CHIRPS), and corresponding skill scores (bias and RMSE)

	OBS	PERSIANN-CDR	CHIRPS 2.0
Mean	52.8	22.5	35.3
Bias		– 30.3	– 17.5
RMSE		31.1	18.9

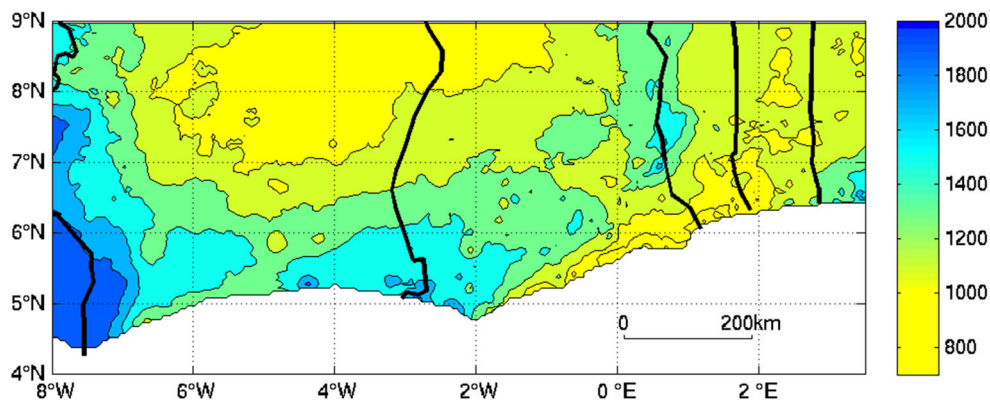
PERSIANN and CHIRPS underestimated P95 amounts as compared to observed rainfall (bias < 0). However, PERSIANN-CDR bias (– 30.3 mm/day) is much larger than that obtained from CHIRPS (– 17.5 mm/day) and its RMSE is 65% higher than that of CHIRPS. It should be noted that for the P99, P90, and P50, the best scores are also obtained with CHIRPS (not shown). The overall median rainfall (P50) in CHIRPS (8.79 mm/day) is actually very close to the observation (8.62 mm/day). Thus, CHIRPS was selected in this study for further application.

### 4.2 Climatology of mean and extreme rainfall

Figure 2 shows the spatial distribution of mean annual rainfall in the region based on CHIRPS data. Mean rainfall values very close to CHIRPS are obtained at the available corresponding stations (not shown), and the rainfall pattern is in very good agreement with published mean annual rainfall maps (e.g. L'Hôte and Mahé 1996). High rainfall is found in the southwest of Côte d'Ivoire along its border with Liberia. Further east in Côte d'Ivoire and southwestern Ghana, between 7 and 2° W, relatively high amounts (1400 to 1600 mm) are found along or close to the coast, and rainfall decreases as one moves away from the coastline. However, between the Cape of Three Points (2° W) and 2° E, the coastal region is much drier (below 1000 mm), and by contrast to Côte d'Ivoire, rainfall increases as one moves away from the coastline. East of 2° E, the dry area extends inland in the “diagonale de sécheresse” (dry corridor) depicted by several authors (Boko 1988; Bokonon–Ganta 1987).

The spatial patterns of P95 are shown in Fig. 3a and b, for the rain gauge data and for CHIRPS, respectively. It should be emphasized that the spatial pattern obtained using other extreme value threshold such as P90 and P99 is identical with that of the P95 threshold. Observed P95 values singularize the coastal region, where high values are found (50–85 mm/day), whereas inland stations almost all show values below 50 mm/day. Within the coastal belt, particularly high values are found west of 2° W (Côte d'Ivoire and western Ghana). In CHIRPS, we notice a systematic negative bias as depicted above. On average, the P95 values are – 15 mm/day lower in CHIRPS than at rain gauge stations. This bias can be explained by the

**Fig. 2** Mean annual rainfall (mm) during 1981–2015 from CHIRPS data



method used to obtain the daily rainfall estimates based on daily values of the Coupled Forecast System version 2 (Funk et al. 2015).

However, there are similarities in the spatial patterns displayed by the two datasets. As in the observation, high P95 values are found on the coastline in CHIRPS, at least in Côte d’Ivoire and western Ghana (about 45–64 mm/day) and lower ones on the continent (about 25–40 mm/day). The difference between the coast and the interior is less pronounced along the eastern part of the region, where the coastal belt is drier. On the whole, these results suggest higher rainfall intensities on the coast, with a secondary differentiation between the western coast (higher intensities west of 2° W) and the eastern coast.

Mean monthly rainfall and monthly values of P95 are plotted in Fig. 4. Given the differences noted above between the coastal belt and the inland areas in terms of rainfall intensity,

two plots are built, the first one for the spatial average of all inland stations, the second one for the average of all coastal stations (listed in Table 1).

In the interior of the continent, there is a very weak bimodal regime (see Fig. 4), whereas at the coastal stations, there are two well-differentiated rainy seasons (the main one from April to July and the smaller one from September to November). Figure 4 also shows an interesting demarcation between coastal and inland stations in terms of rainfall intensity, as denoted by P95. Inland stations (Fig. 4a) do not show much intermonthly variation of P95 (around 40–50 mm/day throughout the year). It is an indication that rainfall intensity (when it rains) is stable throughout the year at continental stations.

However, at the coastal stations (Fig. 4b), there is a large seasonal variation of P95. The lowest and highest values are recorded in August (38 mm/day) and June (82 mm/day),

**Fig. 3** Ninety-fifth percentile of daily rainfall over the period 1981–2015. **a** Rain gauges. **b** CHIRPS. Units: mm/day

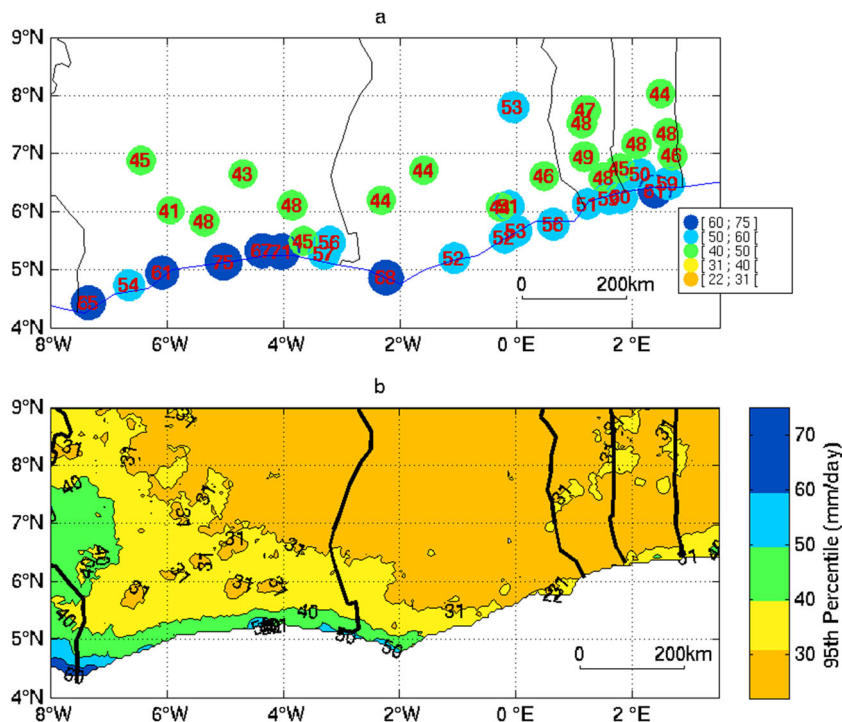
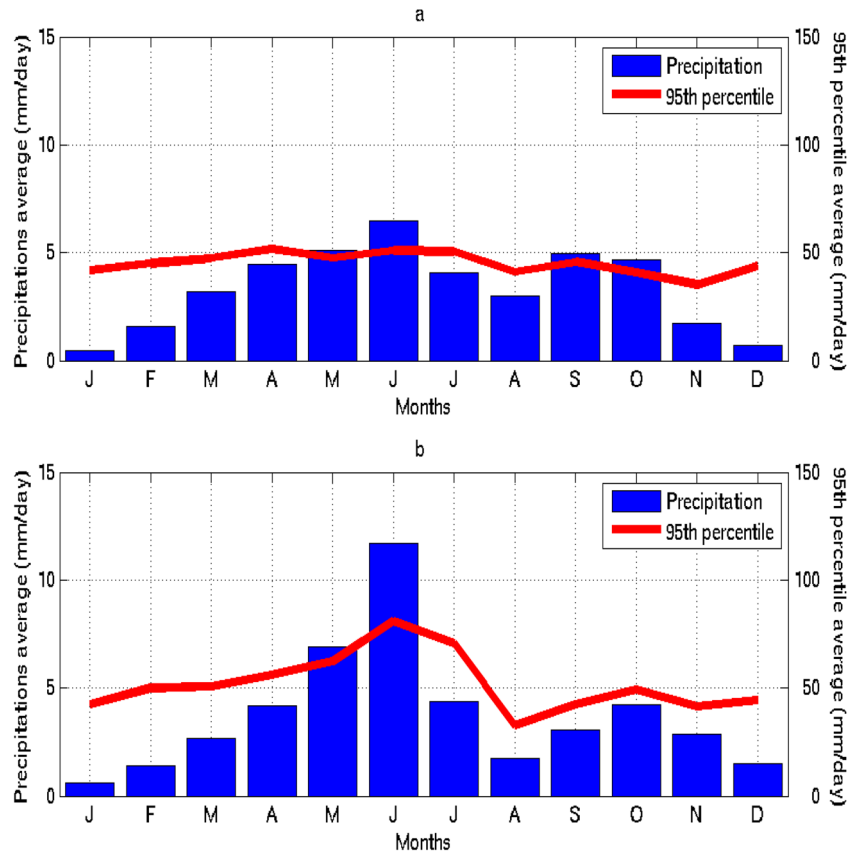




**Fig. 4** Mean monthly precipitation and 95th percentile for the 19 continental stations (a) and for the 19 coastal stations (b), 1981–2015



respectively. More generally, the 3 months, May, June, and July, show a much higher rainfall intensity in the coastline area than inland. This high seasonal variability of extreme rainfall along the coast partly corresponds to the bimodality of the precipitation regimes, with the main rain season coinciding with the period of highest rainfall intensity, whereas inland, there is no relationship between the precipitation regime and rainfall intensity. These observations confirm the specificity of the southern coast of West Africa and show that the most extreme precipitation recorded is mainly from May to July, while in August, precipitation is low (due to air cooling caused by coastal upwelling, inhibiting convection) and less extreme. Note that the western and eastern parts of the SCWA display quite similar seasonal patterns for both mean rainfall and P95, except that the west coast is wetter than the east coast (not show).

### 4.3 Space-time patterns of rainfall variability (1981–2000)

The space-time patterns of annual rainfall totals are first investigated over the period 1981–2000, for both the rain gauge data and the CHIRPS data, using PPCA. For CHIRPS, principal components are computed from the grid points corresponding to the stations only and not from the full dataset. Table 3 presents the percentage of variances of the first

principal component (PC1) for total rainfall and NP95 for the period 1981–2000 (and 1981–2015 for CHIRPS).

It has been decided to retain only PC1 because PC2 explains a much smaller percentage of variance and is of comparatively little interest. The results obtained with PP95 are not shown, since the variance explained by PC1 on rain gauge is low. This is likely due to the fact that, given the relatively small number of stations, there is high spatial variation in the exact rainfall amount recorded on extreme rain days.

Table 3 indicates a high spatial covariability of total rainfall for the two rainfall datasets. However, this covariability is smaller for rain gauge data (42.3% of variance explained by PC1) than for CHIRPS (59% of variance over the same period 1981–2000). This could be expected since in gridded datasets such as CHIRPS, there is a spatial smoothing of the data which tends to increase the signal-to-noise ratio. The slight

**Table 3** Percentage of variances of principal component 1 calculated on total rainfall and NP95 for the 1981–2000 and 1981–2015 periods

	Total rainfall	NP95
Observation (1981–2000)	42.31%	24.51%
CHIRPS (1981–2000)	59.04%	44.85%
CHIRPS (1981–2015)	55.51%	43%

differences in rainfall covariability between the two datasets are confirmed in Fig. 5b and d. Figure 5d indicates that while all CHIRPS grid points are strongly correlated (0.6 to 0.9) with PC1, correlations are mostly lower in observations (Fig. 5b). Station coordinates generally exceed 0.6 over the eastern coastal area, with slightly smaller values inland; most rainfall stations over coastal Côte d'Ivoire are poorly described by PC1. On the whole, however, it is found that PC1 has a fairly uniform signal over much of the region (except in the westmost part for rain gauge data) in both datasets.

Figure 5a and c show that there is a good agreement between the time series associated with PC1 for the observations and CHIRPS, with major dry years found in 1983, 1986, 1992, 1998, and 2000 in the two datasets. This is confirmed by the very high correlation coefficient between PC1 from observations and CHIRPS ( $r = 0.88$ ), which is significant at the 95% threshold. It can be concluded that CHIRPS's dominant pattern of total rainfall covariability replicates the observations.

The same analysis is carried out with NP95 (Fig. 6). For observed data, all stations (except coastal Ivorian stations) are positively correlated with PC1, with a majority of coefficients in the range of 0.3 to 0.6 (Fig. 6b). A moderate NP95 covariability is found across Benin, Togo, Ghana, and continental Côte d'Ivoire. NP95 for the corresponding CHIRPS grid points displays a stronger spatial coherence, as shown by the fact that all correlations are between 0.5 and 0.9. This difference between the two datasets is reflected in the variance explained by PC1 (Table 3, 24.51% and 44.85% for Observations and CHIRPS, respectively).

However, there is a highly positive correlation ( $r = 0.61$ , significant at the 95% level) between the NP95 PC1 scores from the observed and CHIRPS data. Similar variations are observed for several years in the two standardized PC1 anomalies (Fig. 6a and c) during the 1981–2000 period. The years

1983, 1990, 1992, 1998, and 2000 stand out as having a small number of extreme rainfall events in both datasets over most of the region. On the whole, the PC1 obtained from CHIRPS and observations depict quite a similar signal, covering much of the region. CHIRPS is a good substitute to observations during this period.

Considering the good accordance between rain gauge observation and CHIRPS during 1981–2000, CHIRPS is now used for studying trends of parameters (total rainfall, NP95, PP95, NL95, PL95) during the longer 1981–2015 period and over the whole region.

#### 4.4 Rainfall trends (1981–2015)

The trends of total rainfall, NP95, PP95, NL95, and PL95, have been determined for each grid-point and mapped (Fig. 7).

The map for total rainfall (Fig. 7a) points out two cases: regions where total rainfall increases (southern and western parts of Côte d'Ivoire and southern part of Benin and Togo) and regions where total rainfall is generally stable with only a few highly localized grid points in southern Ghana showing a rainfall decrease. An analysis of the other rainfall variables shows that these trends in total rainfall conceal several different situations.

Several coastal and inland areas of Benin, Togo, Ghana, and Ivory Coast recorded an increase/decrease in NP95/NL95, respectively, in the 1981–2015 period (Fig. 7b and d). In Fig. 7c and e, it is noticed an increase/decrease of PP95/PL95, respectively, in several coastal and inland areas (for PL95, the downward trend is clear in southern Ghana).

In western and southern Côte d'Ivoire and Togo/Benin, the upward trend in total rainfall is therefore mainly associated with a larger number of extreme rainfall; hence, the contribution of extreme rainfall to annual rainfall increases. Southern

**Fig. 5** PPCA of total rainfall for 1981–2000, for observed (top panels) and CHIRPS grid points corresponding to station coordinates (bottom panels). Standardized anomalies of the first component (PC1): panels (a) and (c). Correlation coefficients between rainfall and PC1: panels (b) and (d)

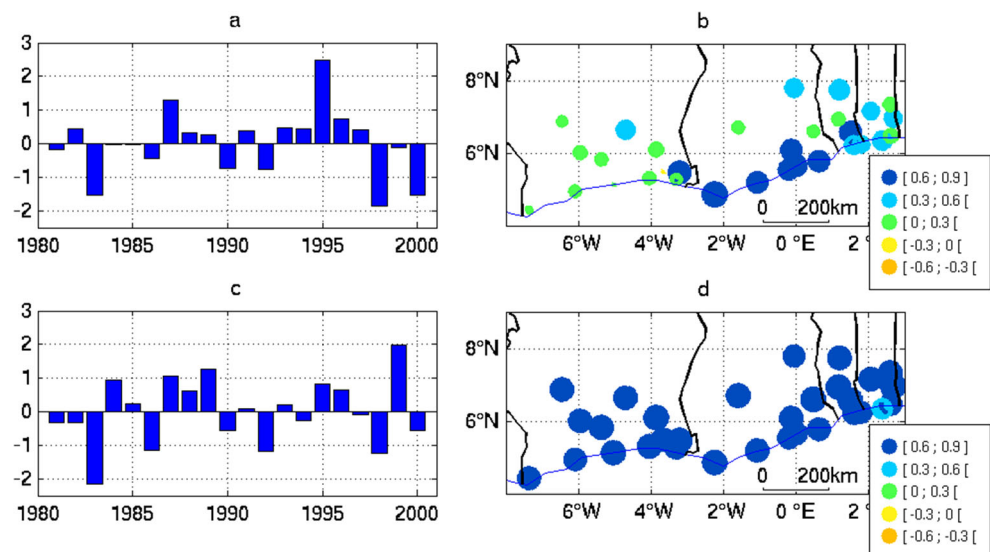
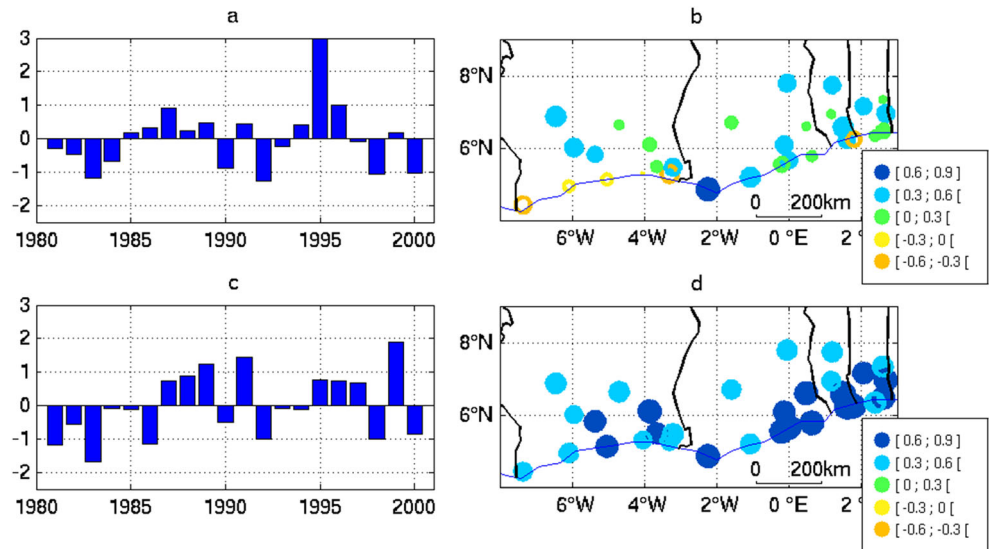


**Fig. 6** PPCA of stations and CHIRPS for NP95 for 1981–2000. **a** Standardized anomalies of the first component (CP1) and **b** correlation coefficients between CP1 and stations. **c** and **d** The same for CHIRPS grid-point corresponding to station coordinates



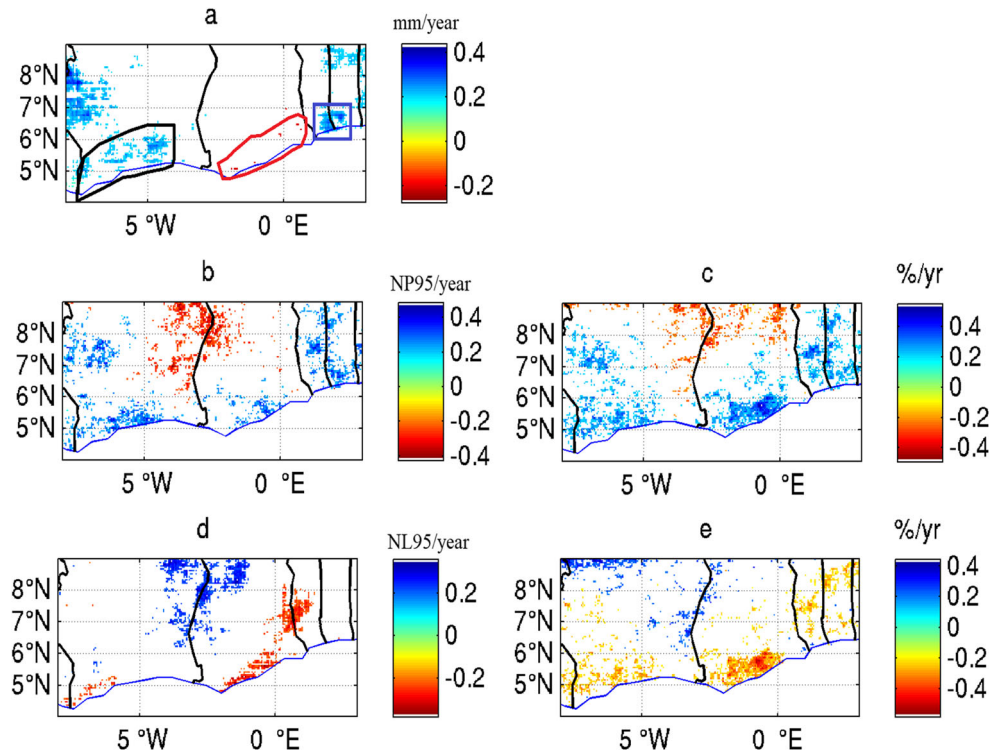
Ghana, despite an increase of NP95, recorded a strong significant decrease of NL95. These opposite trends result in a relative stability of total rainfall (Fig. 7a), although with an increasing (decreasing) contribution of NP95 (NL95) to the annual rainfall total (Fig. 7c and e, respectively).

Rainfall analysis in the 1981–2015 period with CHIRPS revealed different regional trend patterns. To further explore these trends, we calculate 3 regional indices (Southern and Western Côte d’Ivoire (box 1), Southern Ghana (box 2), and Southern Togo/Benin (box 3)) for both CHIRPS and rain gauges. The regional indices are computed for each rainfall

variable (total rainfall, NP95, PP95, NL95, and PL95). The comparison between CHIRPS and rain gauges is based on a graphical analysis of interannual anomaly time series (Fig. 8), the calculation of Pearson correlation coefficients (Table 4), and trend assessment using the Mann-Kendall test and Sen’s method (Table 5).

In western and southern Côte d’Ivoire (“box 1”, black polygon in Fig. 7a), Fig. 8 a to e show a reasonable agreement between the observation (rain gauge (RG)) and CHIRPS, as confirmed in Table 4. The Pearson correlation coefficient (0.49) between CHIRPS and RG exceeds 95% significance

**Fig. 7** Trends of total rainfall (a), NP95 (b), PP95 (c), NL95 (d), and PL95 (e) in the 1981–2015 period with CHIRPS datasets. Pixels shown are significant at 90% according to the test of Mann-Kendall. Trend magnitudes are obtained using Sen’s method. The black polygon, red polygon, and blue rectangle delimit geographical areas where consistent and significant trends are recorded for some of the variables and whose time series are plotted in Figs. 8



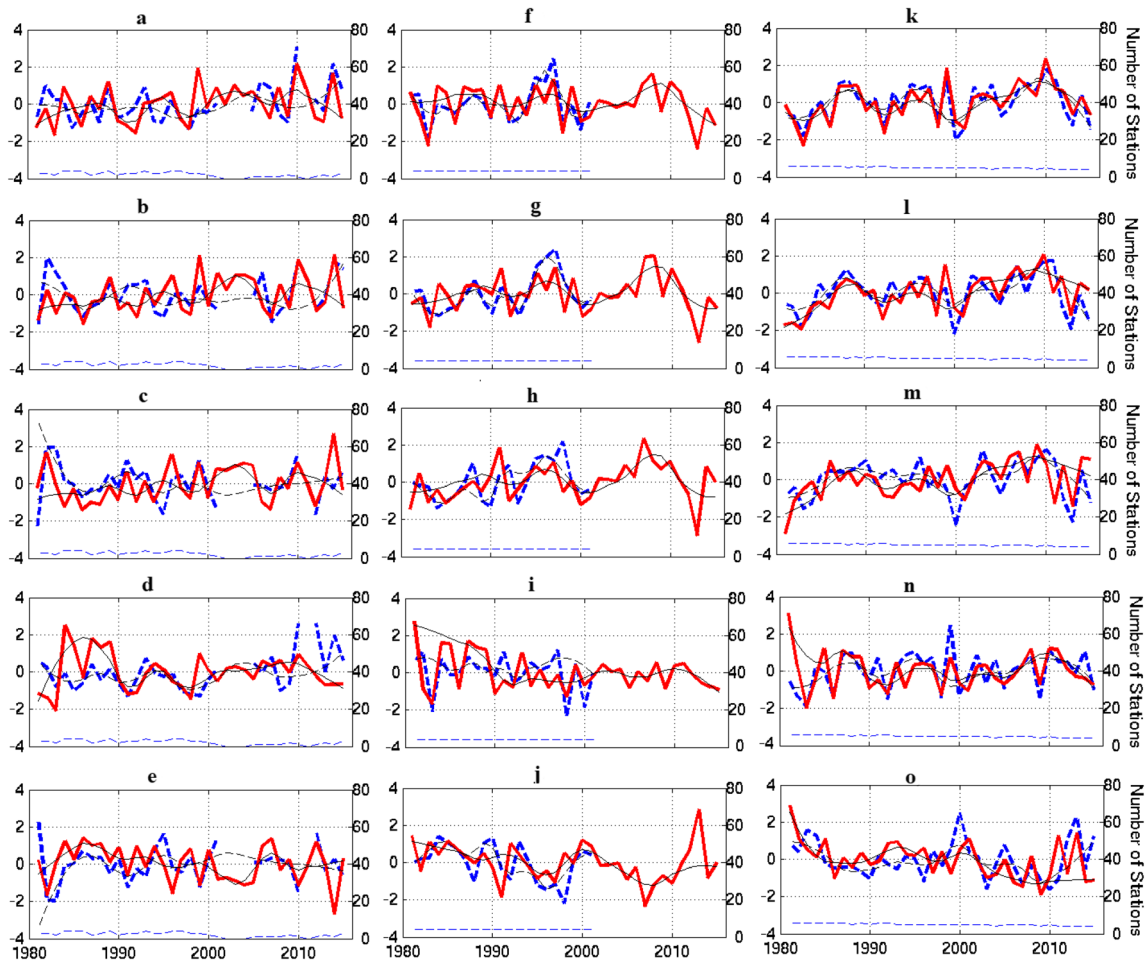


**Fig. 8** Time series of standardized anomalies for total rainfall (a, f, k), NP95 (b, g, l), PP95 (c, h, m), NL95 (d, i, n), and PL95 (e, j, o) in the period 1981–2015 using CHIRPS (solid red line) and rain gauge (dashed blue line) for southern and western parts of Côte d’Ivoire (corresponding to box 1) (left column), for southern Ghana (corresponding to box 2)

(middle column) and for southern Togo/Benin (corresponding to box 3) (right column). Thin black lines: smoothed variations using loess regression for CHIRPS (solid) and rain gauge (dashed) datasets. Thin dashed blue line: number of stations by year

for all indices except for NL95. All indices in the two datasets show large interannual variations (Fig. 8). Table 5 reveals that RG trends of total rainfall, NP95, NL95, and PL95 are all

positive but not significant. In CHIRPS, there is a significantly (at 5% significance level) positive trend for total rainfall, but for NP95, PP95, and NL95, the trend is positive but not significant. The direction of trends is therefore similar between the two datasets for all indices except PP95 and PL95, which could be due to the fact that some years are missing in the RG time series. However, trends are weak in this region.

**Table 4** Pearson correlation coefficient between rain gauges and CHIRPS pixels for each box for total rainfall, NP95, PP95, NL95, and PL95. Box 1, box 2, and box 3 are regional indices averaging all rain gauges and CHIRPS pixels located in western and southern parts of Côte d’Ivoire, Southern Ghana, and Southern Togo/Benin, respectively, as shown in Fig. 7. Values in italics are statistically significant at the 5% significance level

	Box 1	Box 2	Box 3
Total rainfall	<i>0.49</i>	<i>0.73</i>	<i>0.88</i>
NP95	<i>0.44</i>	<i>0.49</i>	<i>0.68</i>
PP95	<i>0.36</i>	<i>0.34</i>	<i>0.34</i>
NL95	0.07	<i>0.44</i>	<i>0.52</i>
PL95	<i>0.36</i>	<i>0.34</i>	<i>0.34</i>

Figure 8 f to j show the indices extracted for southern Ghana (“box 2”, red polygon in Fig. 7a). The agreement between RG and CHIRPS time series is fair for this region during the common period 1981–2001. All Pearson correlation coefficients are significant (5% significance level, Table 4) and the maximum is recorded for total rainfall ( $R = 0.73$ ). In the 1981–2001 period, the sign of Sen’s coefficient’s for NP95, PP95, NL95, and PL95 is the same for both datasets. This makes us confident in the use of the southern Ghana rainfall indices derived from CHIRPS in the 1981–2015 period. The regional index confirms the absence of a clear trend in total rainfall. However, there are positive and negative trends

**Table 5** Trend statistics (1981–2015) for each rainfall index (total rainfall, NP95, PP95, NL95, and PL95) for rain gauge (RG) and CHIRPS in western and southern Côte d’Ivoire (box 1), Southern Ghana (box 2), and Southern Togo/Benin (box 3). Values are Sen’s

	Box 1		Box 2			Box 3	
	RG	CHIRPS	RG (1981–2001)	CHIRPS_G (1981–2001)	CHIRPS	RG	CHIRPS
Total rainfall	0.02	<i>0.03</i>	0.01	–0.01	–0.01	0.02	<i>0.03</i>
NP95	0.01	0.02	0.05	0.03	0.01	0.02	<i>0.05</i>
PP95	–0.01	0.03	0.06	0.04	<i>0.03</i>	0.01	<i>0.05</i>
NL95	0.02	0.01	–0.02	–0.08	–0.03	0.02	–0.01
PL95	0.01	–0.03	–0.06	–0.04	– <i>0.03</i>	–0.01	– <i>0.05</i>

(significant at the 5% level) in PP95 and PL95, respectively, which demonstrate that extreme rainfall events gradually contribute to a higher share of the total rainfall amount in southern Ghana, although some years like 2013 demarcate from this pattern (Fig. 7c and e). On both the 1981–2001 and 1981–2015 periods, there are also decadal variations for all indices in southern Ghana.

In southern Togo/Benin (“box 3”, blue rectangle in Fig. 7a), the accordance between the time series associated for the observations and CHIRPS in western Togo/Benin is generally good (see Fig. 8 k to o and Table 4) for each index ( $r = 0.88$  for total rainfall). In the period 1981–2015, all indices show large interannual as well as decadal variations (Fig. 8). For all indices (excepted PL95), the decadal variation has two positive phases (1985–1990 and 2003–2013) and two negative phases in the early 1990s and early 2000s. These decadal variations tend to lower the statistical significance of linear trends. In CHIRPS datasets, there are significantly (at 5% level) positive trends for total rainfall, NP95, and PP95 and a negative trend for NL95 and PL95 (Table 5). Although the 5% significance is not reached, the signs of Sen’s coefficient for rain gauge data are the same as for CHIRPS for total rainfall, NP95, PP95, and PL95. For NL95, the opposite signs noticed in Table 5 are explained by the very large number of non-extreme rainfall events in CHIRPS in 1981 (Fig. 8n), which affected the trend of NL95. These results confirm the observations made from Fig. 7 that the rainfall increase in southern Togo/Benin is mostly due to more and stronger extreme rainfall events.

However, a closer comparison of the time series reveals that the relationship between total rainfall and rainfall intensity is not straightforward. The two wet years 1999 and 2010 in southern Togo/Benin (Fig. 8k) are induced by a large number of non-extreme and extreme rainfall events, respectively (Fig. 8l and n). As a result, the contribution of non-extreme rainfall to total rainfall is very high in 1999 while extreme rainfall mostly contributes to the high total rainfall in 2010 (Fig. 8m and o). It therefore merges that there are two classes of wet years, those associated with several extreme rainfall events

slope coefficients. Significant trend values at the 5% significance level are in italics. CHIRPS\_G designates CHIRPS trend in the 1981–2001 to match Ghana rain gauge data availability

and those caused by a large number of low-intensity rainfall events. Similarly, two categories of dry years are found: (i) those like 1983, 2000, and 2013, associated with a deficit of extreme rainfall events (Fig. 8l) combined to low contribution of extreme rainfall in the total rainfall (Fig. 8m); (ii) those like 1992 and 1998 which recorded a normal number of extreme rainfall events (Fig. 8l), but a small number of non-extreme rainfall events (Fig. 8n). These case studies, together with diverse trends of the rainfall variables, show that the interpretation of trends in total rainfall is not trivial.

## 5 Discussion and conclusion

The present study investigated the patterns and trends (1981–2015) of extreme rainfall over the southern coastal belt of West Africa. To achieve this work, rain gauge data have been supplemented by satellite rainfall estimates. An evaluation was carried out of three daily rainfall estimation products (TRMM, PERSIANN, and CHIRPS) with respect to their performance at reproducing the 95th percentile of daily rainfall amounts, which is retained to depict the extreme events. TRMM shows the best performance, followed by CHIRPS. Because of its longer period of record (1981–2015) and higher spatial resolution, the CHIRPS dataset was selected as an alternative dataset to rain gauges.

It emerges that rainfall on the littoral zone of southern West Africa is more extreme than inland. Previous studies noticed higher values of daily rainfall in the southern part of Côte d’Ivoire (Goula et al. 2007; Soro et al. 2016) and Benin (Ague and Afouda 2015). The contribution of the current study is to show that despite its low annual rainfall, the coastal belt of Ghana and Togo also exhibits quite heavy rainfall events, in continuity with those of Côte d’Ivoire and Benin. The present study showed that the higher rainfall intensities of coastal southern West Africa are mainly recorded from May to July.

Variation in extreme rainfall during the 1981–2015 period on the Southern coastal belt of West Africa were examined by

mapping linear trends for different rainfall indicators using CHIRPS data. The findings were confirmed by computing regional indices from rain gauges over selected sub-regions. Two cases were detected:

- In the southern and western parts of Côte d’Ivoire and the southern part of Togo/Benin, there is an increase in total rainfall mainly explained by an increasing number of extreme rainfall whereas the number of days with rainfall less than P95 does not change. The percentage rainfall amount on extreme rainfall days compared to the total rainfall therefore increases, while there is a decrease of the percentage of total rainfall on days receiving less than P95 compared to the total annual rainfall. These trends are best shown in Togo/Benin CHIRPS data;
- In the southern part of Ghana, CHIRPS shows a stable total rainfall due to an increase in the number of extreme rainfall days compensated by a decrease in the number of days with rainfall less than P95. As a result, the percentage rainfall accounted for by extreme rainfall events increases while the percentage rainfall accounted for by lower intensity precipitation decreases. A similar pattern (an increase of the number of extreme rainfall while the total rainfall amount remains stable) has been described in Manzanas et al. (2014) over southern Ghana during the 1984–2010 period.

Furthermore, the present study shows that trends are homogeneously significant and they are masked by a strong interannual and decadal variability of all indices in the 1981–2015 period (mostly over the eastern part of the region) without any clear differentiation between the coastal and inland areas.

These results are broadly consistent with earlier results obtained for the Guinean climatic region of West Africa (Goula et al. 2012; Odoulami and Akinsanola 2017) where trends were found to be weaker and spatially less consistent than those found in Sahel (Chaney et al. 2014; Panthou et al. 2014; Sanogo et al. 2015; Barry et al. 2018). The present study suggests that the large interannual variability of the number of extreme rainfall and their contribution on total rainfall in the 1981–2015 period weakens the long-term trend. Furthermore, some decadal variations tend to overshadow long-term trends, and the local evolution of extreme rainfall also sometimes differs significantly from the regional trends. Finally, despite the higher average intensity of daily rainfall in the littoral belt, this area differs little from the interior regions in terms of trends.

It can be hypothesized that the increase in the frequency of extreme rainfall observed in part of the region (although moderate) is linked to the intensification of the hydrological cycle which was shown to result from global climate warming (IPCC 2013). This trend, added to the higher intensity of

rainfall in the coastal region, makes flood hazards a major threat along the coast. This should be considered in a context of increased vulnerability because of deficient urban planning policies in this region.

Further investigations are needed to elucidate the origin of this particularity of the coastal belt marked by extreme rainfall especially in the May–July season. While Leduc-Leballeur et al. (2013) pointed to the role of sea surface temperature gradients on a low atmospheric local circulation (LALC) in the occurrence of seasonal extreme rainfall in the SCWA, a better appraisal of the atmospheric disturbances associated with these extreme rainfall events and their interaction with sea breezes would be crucial.

**Acknowledgements** The authors are very thankful to Dr. Ernest Amoussou for providing the Togo gauge data.

**Funding** This document was produced with the financial support of the Prince Albert II of Monaco Foundation.

The contents of this document are solely the liability of Mr. Marc Kpanon and under no circumstances may be considered a reflection of the position of the Prince Albert II of Monaco Foundation and/or the IPCC.

## References

- Adler RF, Negri AJ (1988) A satellite infrared technique to estimate tropical convective and Stratiform rainfall. *J Appl Meteorol* 27:30–51. [https://doi.org/10.1175/1520-0450\(1988\)027<0030:ASITTE>2.0.CO;2](https://doi.org/10.1175/1520-0450(1988)027<0030:ASITTE>2.0.CO;2)
- Ague AI, Afouda A (2015) Analyse fréquentielle et nouvelle cartographie des maxima annuels de pluies journalières au Bénin. *Int J Biol Chem Sci* 9(1):121–133. <https://doi.org/10.4314/ijbcs.v9i1.12>
- Aguilar E, Aziz Barry A, Brunet M, Ekang L, Fernandes A, Massoukina M, Mbah J, Mhanda A, do Nascimento DJ, Peterson TC, Thamba Umba O, Tomou M, Zhang X (2009) Changes in temperature and precipitation extremes in western Central Africa, Guinea Conakry, and Zimbabwe. *J Geophys Res-Atmos* 114(D2):1955–2006. <https://doi.org/10.1029/2008JD011010>
- Ashouri H, Hsu KL, Sorooshian S, Braithwaite DK, Knapp KR, Cecil LD, Nelson BR, Prat OP (2015) PERSIANN-CDR: daily precipitation climate data record from multisatellite observations for hydrological and climate studies. *Bull Am Meteorol Soc* 96(1):69–83. <https://doi.org/10.1175/BAMS-D-13-00068.1>
- Bai L, Shi C, Li L, Yang Y, Wu J (2018) Accuracy of CHIRPS satellite-rainfall products over mainland China. *Remote Sens* 10(3):362. <https://doi.org/10.3390/rs10030362>
- Barry AA, Caesar J, Klein Tank AMG, Aguilar E, McSweeney C, Cyrille AM, Nikiema MP, Narcisse KB, Sima F, Stafford G, Touray LM, Ayilari-Naa JA, Mendes CL, Tounkara M, Gar-Glahn EVS, Coulibaly MS, Dieh MF, Mouhaimouni M, Oyegade JA, Sambou E, Laogbessi ET (2018) West Africa climate extremes and climate change indices. *Int J Climatol* 38:921–938. <https://doi.org/10.1002/joc.5420>
- Bayissa Y, Tadesse T, Demisse G, Shiferaw A (2017) Evaluation of satellite-based rainfall estimates and application to monitor meteorological drought for the upper Blue Nile Basin, Ethiopia. *Remote Sens* 9(7):669. <https://doi.org/10.3390/rs9070669>

- Boko M (1988) Climat et communautés rurales du Bénin : Rythmes climatiques et rythme de développement. Thèse d'Etat ès lettres, Dijon 607 p
- Bokonon-Ganta E (1987) Les climats de la région du Golfe de Guinée. Thèse de Doctorat du 3ème cycle. Institut de Géographie, Université de Paris-Sorbonne, Paris, 248 p + annexe
- Chaney NW, Sheffield J, Villarini G, Wood EF (2014) Development of a high-resolution gridded daily meteorological dataset over sub-Saharan Africa: spatial analysis of trends in climate extremes. *J Clim* 27(15):5815–5835. <https://doi.org/10.1175/JCLI-D-13-00423.1>
- Dembélé M, Zwart SJ (2016) Evaluation and comparison of satellite-based rainfall products in Burkina Faso, West Africa. *Int J Remote Sens* 37(17):3995–4014. <https://doi.org/10.1080/01431161.2016.1207258>
- Erman A, Motte E, Goyal R, Asare A, Takamatsu S, Chen X, Malgioglio S, Skinner A, Yoshida N, Hallegatte S (2018) The road to recovery: the role of poverty in the exposure, vulnerability, and resilience to floods in Accra. The World Bank, Washington, D.C.
- Funk C, Peterson P, Landsfeld M, Pedreros D, Verdin J, Shukla S, Husak G, Rowland J, Harrison L, Hoell A, Michaelsen J (2015) The climate hazards infrared precipitation with stations—a new environmental record for monitoring extremes. *Scientific Data* 2:150066. <https://doi.org/10.1038/sdata.2015.66>
- Gocic M, Trajkovic S (2013) Analysis of changes in meteorological variables using Mann-Kendall and Sen's slope estimator statistical tests in Serbia. *Glob Planet Chang* 100:172–182. <https://doi.org/10.1016/j.gloplacha.2012.10.014>
- Goula BT, Brou K, Brou T, Savane I, Vamoryba F, Bernard S (2007) Estimation des pluies exceptionnelles journalières en zone tropicale: cas de la Côte d'Ivoire par comparaison des lois Lognormale et de Gumbel. *Hydrol Sci J—des Sciences Hydrologiques* 52(1):49–67. <https://doi.org/10.1623/hysj.52.1.49>
- Goula BTA, Soro EG, Kouassi W, Srohourou B (2012) Tendances et ruptures au niveau des pluies journalières extrêmes en Côte d'Ivoire (Afrique de l'Ouest). *Hydrol Sci J* 57:1067–1080. <https://doi.org/10.1080/02626667.2012.692880>
- Groisman PY, Knight RW, Easterling DR, Karl TR, Hegerl GC, Razuvayev VN (2005) Trends in extreme precipitation in the climate record. *J Clim* 18(9):1326–1350. <https://doi.org/10.1175/JCLI3339.1>
- Herold N, Behrangi A, Alexander LV (2017) Large uncertainties in observed daily precipitation extremes over land. *J Geophys Res-Atmos* 122(2):668–681. <https://doi.org/10.1002/2016JD025842>
- IPCC Climatic Change (2013) The physical science basis. Contribution of Working Group I to the Fifth Assessment Report of the Intergovernmental Panel on Climate Change. Cambridge University Press, Cambridge
- Katsanos D, Retalis A, Michaelides S (2016) Validation of a high-resolution precipitation database (CHIRPS) over Cyprus for a 30-year period. *Atmos Res* 169:459–464. <https://doi.org/10.1016/j.atmosres.2015.05.015>
- Kendall MG (1975) Rank correlation methods. Griffin, London
- L'Hôte Y, Mahé G (1996) Afrique de l'ouest et centrale : précipitations moyennes annuelles (période 1951-1989). West and Central Africa: mean annual rainfall (1951-1989). ORSTOM, Paris
- Leduc-Leballeur M, De Coëtlogon G, Eymard L (2013) Air–sea interaction in the Gulf of Guinea at intraseasonal time-scales: wind bursts and coastal precipitation in boreal spring. *Q J R Meteorol Soc* 139(671):387–400. <https://doi.org/10.1002/qj.1981>
- Li JG, Ruan HX, Li JR, Huang SF (2010) Application of TRMM precipitation data in meteorological drought monitoring. *J China Hydrol* 30(4):43–46
- Lopes AV, Chiang JCH, Thompson SA, Dracup JA (2016) Trend and uncertainty in spatial-temporal patterns of hydrological droughts in the Amazon basin. *Geophys Res Lett* 43(7):3307–3316. <https://doi.org/10.1002/2016GL067738>
- Mann HB (1945) Nonparametric tests against trend. *Econometrica* 13(3): 245–259. <https://doi.org/10.2307/1907187>
- Manzanas R, Amekudzi LK, Preko K, Herrera S, Gutiérrez JM (2014) Precipitation variability and trends in Ghana: an intercomparison of observational and reanalysis products. *Clim Chang* 124(4):805–819. <https://doi.org/10.1007/s10584-014-1100-9>
- Menne MJ, Durre I, Vose RS, Gleason BE, Houston TG (2012) An overview of the global historical climatology network-daily database. *J Atmos Ocean Technol* 29(7):897–910. <https://doi.org/10.1175/JTECH-D-11-00103.1>
- Moron V, Oueslati B, Pohl B, Rome S, Janicot S (2016) Trends of mean temperatures and warm extremes in northern tropical Africa (1961–2014) from observed and PPCA-reconstructed time series. *J Geophys Res Atmos* 121:5298–5319. <https://doi.org/10.1002/2015JD024303>
- Mouhamed L, Traore SB, Alhassane A, Sarr B (2013) Evolution of some observed climate extremes in the West African Sahel. *Weather and climate extremes* 1:19-25.
- Neumann R, Jung G, Laux P, Kunstmann H (2007) Climate trends of temperature, precipitation and river discharge in the Volta Basin of West Africa. *Int J River Basin Manag* 5(1):17–30. <https://doi.org/10.1080/15715124.2007.9635302>
- New M, Hewitson B, Stephenson DB, Tsiga A, Kruger A, Manhique A, Gomez B, Coelho CAS, Masisi DN, Kululanga E, Mbambalala E, Adesina F, Saleh H, Kanyanga J, Adosi J, Bulane L, Fortunata L, Mdoka ML, Lajoie R (2006) Evidence of trends in daily climate extremes over southern and West Africa. *J Geophys Res-Atmos* 111(D14). <https://doi.org/10.1029/2005JD006289>
- Novella N, and Thiaw W (2010) Validation of satellite-derived rainfall products over the Sahel. Wyle Information Systems/CPC/NOAA. p. 1-9
- Odoulami RC, Akinsanola AA (2017) Recent assessment of West African summer monsoon daily rainfall trends. *Weather* 73(9): 283–287. <https://doi.org/10.1002/wea.2965>
- Panthou G, Vischel T, Lebel T (2014) Recent trends in the regime of extreme rainfall in the Central Sahel. *Int J Climatol* 34(15):3998–4006. <https://doi.org/10.1002/joc.3984>
- Sanogo S, Fink AH, Omosho JA, Ba A, Redl R, Ermert V (2015) Spatio-temporal characteristics of the recent rainfall recovery in West Africa. *Int J Climatol* 35(15):4589–4605. <https://doi.org/10.1002/joc.4309>
- Sen PK (1968) Estimates of the regression coefficient based on Kendall's tau. *J Am Stat Assoc* 63:1379–1389. <https://doi.org/10.1080/01621459.1968.10480934>
- Soro GE, Dao A, Fadika V, Goula Bi TA, Srohourou B (2016) Estimation des pluies journalières extrêmes supérieures à un seuil en climat tropical: cas de la Côte d'Ivoire. *Revue Physio-Géo* 10:211–227. <https://doi.org/10.4000/physio-geo.5011>
- Su F, Hong Y, Lettenmaier DP (2008) Evaluation of TRMM Multisatellite Precipitation Analysis (TMPA) and its utility in hydrologic prediction in the La Plata Basin. *J Hydrometeorol* 9(4): 622–640. <https://doi.org/10.1175/2007JHM944.1>
- Ta S, Kouadio KY, Ali KE, Toualy E, Aman A, Yoroba F (2016) West Africa extreme rainfall events and large-scale ocean surface and atmospheric conditions in the tropical Atlantic. *Adv Meteorol* 2016:14–14. <https://doi.org/10.1155/2016/1940456>
- Tipping ME, Bishop CM (1999) Probabilistic principal component analysis. *J R Stat Soc* 61(3):611–622. <https://doi.org/10.1111/1467-9868.00196>
- Toté C, Patricio D, Boogaard H, van der Wijngaart R, Tamavsky E, Funk C (2015) Evaluation of satellite rainfall estimates for drought and flood monitoring in Mozambique. *Remote Sens* 7(2):1758–1776. <https://doi.org/10.3390/rs70201758>

- Trejo FJP, Barbosa HA, Peñaloza-Murillo MA, Moreno MA, Farías A (2016) Intercomparison of improved satellite rainfall estimation with CHIRPS gridded product and rain gauge data over Venezuela. *Atmósfera* 29(4):323–342. <https://doi.org/10.20937/ATM.2016.29.04.04>
- WMO (2009) Guidelines on analysis of extremes in a changing climate in support of informed decisions for adaptation. World Meteorological Organization, Geneva
- Yabi I, Afouda F (2012) Extreme rainfall years in Benin (West Africa). *Quat Int* 262:39–43. <https://doi.org/10.1016/j.quaint.2010.12.010>
- Zambrano-Bigiarini M, Nauditt A, Birkel C, Verbist K, Ribbe L (2017) Temporal and spatial evaluation of satellite-based rainfall estimates across the complex topographical and climatic gradients of Chile. *Hydrol Earth Syst Sci* 21(2):1295–1320. <https://doi.org/10.5194/hess-21-1295-2017>
- Zhang X, Alexander L, Hegerl GC, Jones P, Tank AK, Peterson TC, Trewin B, Zwiers FW (2011) Indices for monitoring changes in extremes based on daily temperature and precipitation data. *Wiley Interdiscip Rev Clim Chang* 2(6):851–870. <https://doi.org/10.1002/wcc.147>
- Zittis G, Bruggeman A, Camera C, Hadjinicolaou P, Lelieveld J (2017) The added value of convection permitting simulations of extreme precipitation events over the eastern Mediterranean. *Atmospheric Research* 191:20-33